

**Prediction of high Curie-temperature intrinsic ferromagnetic  
semiconductors and quantum anomalous Hall states in  $\text{XBr}_3$  ( $\text{X} = \text{Cu, Ag,$   
 $\text{Au}$ ) monolayers: Supplemental Materials**

Xiaojuan Liu<sup>1</sup>, Jiayong Zhang<sup>2</sup>, Yao Wang<sup>1</sup>, Hairui Bao<sup>1</sup>, Yang Qi<sup>1</sup>, Zhongqin Yang<sup>1,3\*</sup>

<sup>1</sup>*State Key Laboratory of Surface Physics and Department of Physics, Fudan University, Shanghai  
200433, China*

<sup>2</sup>*Jiangsu Key Laboratory of Micro and Nano Heat Fluid Flow Technology and Energy Application,  
School of Physical Science and Technology, Suzhou University of Science and Technology, Suzhou  
215009, China*

<sup>3</sup>*Shanghai Qi Zhi Institute, Shanghai 200030, China*

\*Corresponding author: Email: [zyang@fudan.edu.cn](mailto:zyang@fudan.edu.cn)

**Table. S1.** The total energies per formula unit (in meV) for the monolayer XBr<sub>3</sub> (X = Cu, Ag, Au) with various magnetic structures by using GGA + U functional. The values are relative to the total energy of the FM state of the corresponding monolayer.  $J_1$ ,  $J_2$ , and  $J_3$  represent the NN-, NNN-, and TN-coupling constants (in meV) in the Heisenberg model, respectively. The last column gives the magnetic anisotropy energies per X atom (in meV).

	<b>U<sub>eff</sub></b>	<b>FM</b>	<b>n-AFM</b>	<b>s-AFM</b>	<b>z-AFM</b>	$J_1$	$J_2$	$J_3$	<b>MAE</b>
<b>CuBr<sub>3</sub></b>	2.1	0	212.949	168.913	98.996	17.68	1.72	0.07	1.578
	3.1	0	224.135	176.636	104.225	18.53	1.77	0.14	1.530
	4.1	0	232.969	182.639	108.345	19.20	1.81	0.21	1.497
	5.1	0	240.569	188.114	113.653	19.69	1.91	0.36	1.478
<b>AgBr<sub>3</sub></b>	0.8	0	178.723	167.583	77.003	16.83	2.06	-1.94	1.531
	1.3	0	235.553	175.554	84.196	20.43	0.76	-0.80	1.598
	1.8	0	245.426	183.016	89.455	21.19	0.85	-0.73	1.604
	2.3	0	254.564	189.935	94.039	21.90	0.92	-0.69	1.624
<b>AuBr<sub>3</sub></b>	0.5	0	126.125	91.326	22.358	12.19	-0.39	-1.68	0.386
	1.0	0	140.039	102.493	29.775	13.30	-0.24	-1.63	0.415
	1.5	0	152.603	111.761	38.157	14.14	-0.08	-1.42	0.435

**Table. S2.** The total spin magnetic moments per unit cell (in  $\mu_B$ ) of the monolayer XBr<sub>3</sub> (X = Cu, Ag, Au) and the local magnetic moments (in  $\mu_B$ ) at X or Br atoms in the pristine (the first values) and 5% tensile strained (the second values) structures.

	<b>Total</b>	<b>X</b>	<b>Br</b>
<b>CuBr<sub>3</sub></b>	4 / 4	0.58 / 0.55	0.37 / 0.38
<b>AgBr<sub>3</sub></b>	4 / 4	0.43 / 0.39	0.40 / 0.41
<b>AuBr<sub>3</sub></b>	4 / 4	0.58 / 0.56	0.36 / 0.36

**Table. S3.** Magnetic ground states of  $\text{TM}_3$  ( $\text{TM}$  = transition metal atom and  $\text{A} = \text{F}, \text{Cl}, \text{Br}, \text{I}$ ) type monolayer materials with the similar structure of  $\text{XBr}_3$  ( $\text{X} = \text{Cu}, \text{Ag}, \text{Au}$ ) based on theoretical calculations and also experimental measurements (in italics). The numbers express the  $T_c$  for the FM ground state of the materials. The numbers in bold are our results calculated based on a Heisenberg model. The  $T_c$  values we obtained from an Ising model for  $\text{XBr}_3$  ( $\text{X} = \text{Cu}, \text{Ag}, \text{Au}$ ) are 238 K, 190 K, and 64 K, respectively. The upper corner numbers represent the corresponding references.

	$T_c$ /K	TM	Sc	Ti	V	Cr	Mn	Fe	Co	Ni	Cu
A											
<b>F</b>	-	-	-	-	41 <sup>6</sup>	450 <sup>7</sup>	-	-	-	-	-
<b>Cl</b>	NM <sup>1</sup>	376 <sup>2</sup>	425 <sup>2</sup> (80 <sup>4</sup> )	-	49 <sup>6</sup>	620 <sup>7</sup>	-	-	400 <sup>10</sup> (497 <sup>11</sup> )	74 <sup>12</sup>	-
<b>Br</b>	NM <sup>1</sup>	75 <sup>3</sup>	190 <sup>5</sup>	73 <sup>6</sup> (34 <sup>25</sup> )	73 <sup>6</sup> (34 <sup>25</sup> )	700 <sup>7</sup>	AFM <sup>5</sup>	NM <sup>9</sup>	100 <sup>5</sup> (595 <sup>11</sup> )	<b>149</b>	-
<b>I</b>	NM <sup>1</sup>	90 <sup>3</sup>	98 <sup>4</sup>	95 <sup>6</sup> (45 <sup>26</sup> )	95 <sup>6</sup> (45 <sup>26</sup> )	720 <sup>7</sup>	AFM <sup>8</sup>	-	682 <sup>11</sup>	-	-
	<b>Y</b>	<b>Zr</b>	<b>Nb</b>	<b>Mo</b>	<b>Tc</b>	<b>Ru</b>	<b>Rh</b>	<b>Pd</b>	<b>Ag</b>		
<b>F</b>	-	-	-	-	-	-	-	-	-	-	-
<b>Cl</b>	-	130 <sup>13</sup>	-	-	AFM <sup>14</sup>	-	14 <sup>15</sup>	NM <sup>18</sup>	528 <sup>19</sup>	-	-
<b>Br</b>	NM <sup>1</sup>	-	-	-	AFM <sup>14</sup>	-	13 <sup>16</sup>	NM <sup>18</sup>	110 <sup>5</sup> (350 <sup>20</sup> )	<b>118</b>	-
<b>I</b>	NM <sup>1</sup>	-	-	-	24 <sup>14</sup>	FM <sup>8</sup>	2 <sup>16</sup> (360 <sup>17</sup> )	NM <sup>18</sup>	150 <sup>20</sup>	-	-
	<b>La</b>	<b>Hf</b>	<b>Ta</b>	<b>W</b>	<b>Re</b>	<b>Os</b>	<b>Ir</b>	<b>Pt</b>	<b>Au</b>		
<b>F</b>	-	-	-	-	-	-	-	-	-	-	-
<b>Cl</b>	-	-	-	-	-	-	350 <sup>22</sup>	-	200 <sup>24</sup>	-	-
<b>Br</b>	-	-	-	-	-	390 <sup>21</sup>	-	-	375 <sup>20</sup>	<b>31</b>	-
<b>I</b>	-	-	-	AFM <sup>8</sup>	165 <sup>21</sup>	35 <sup>23</sup>	-	-	164 <sup>20</sup>	-	-

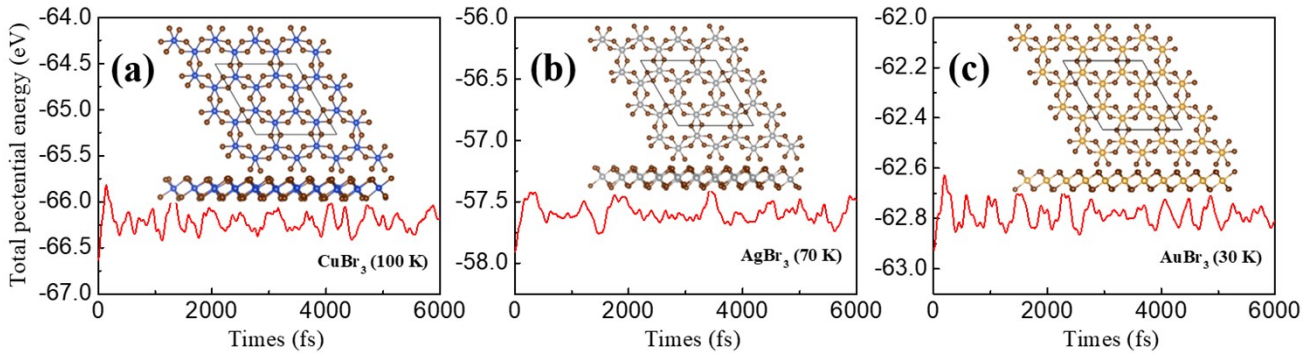


Fig. S1. Total energy fluctuation of the monolayer CuBr<sub>3</sub> at 100 K (a), AgBr<sub>3</sub> at 70 K (b), and AuBr<sub>3</sub> at 30 K (c) during the AIMD simulations. The insets show the corresponding atomic structures for the three monolayers at the end of the simulations.

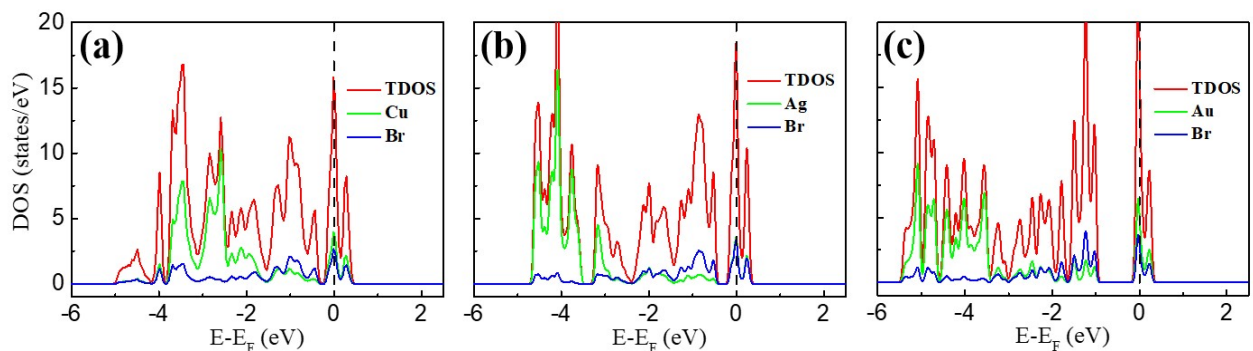


Fig. S2. The calculated total DOSs of the XBr<sub>3</sub> (X = Cu, Ag, Au) monolayers in the non-magnetic state.

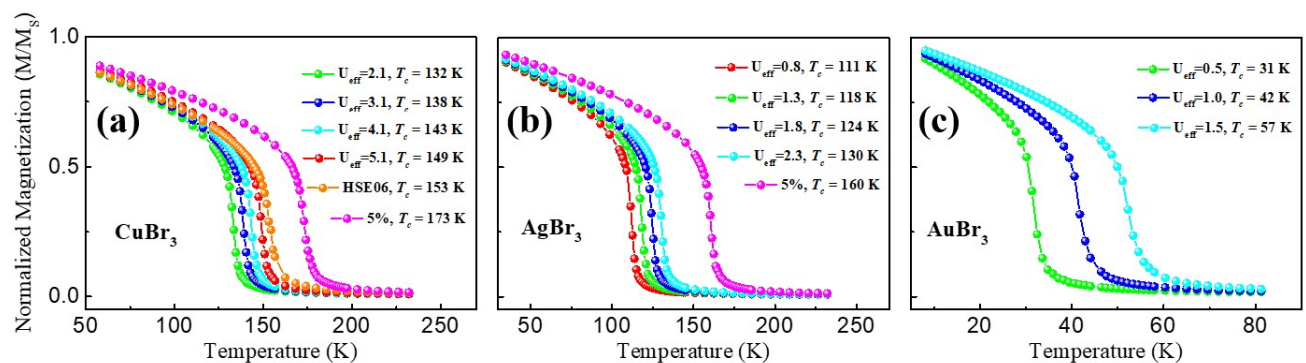


Fig. S3. Monte Carlo simulations on the magnetization for the (a) CuBr<sub>3</sub>, (b) AgBr<sub>3</sub>, and (c) AuBr<sub>3</sub> monolayers with different U<sub>eff</sub> values for the X (Cu, Ag, Au) *d* orbitals. In (a), the HSE06 result is also given. The results for CuBr<sub>3</sub> and AgBr<sub>3</sub> under 5% tensile strain are also displayed in (a) and (b), respectively.

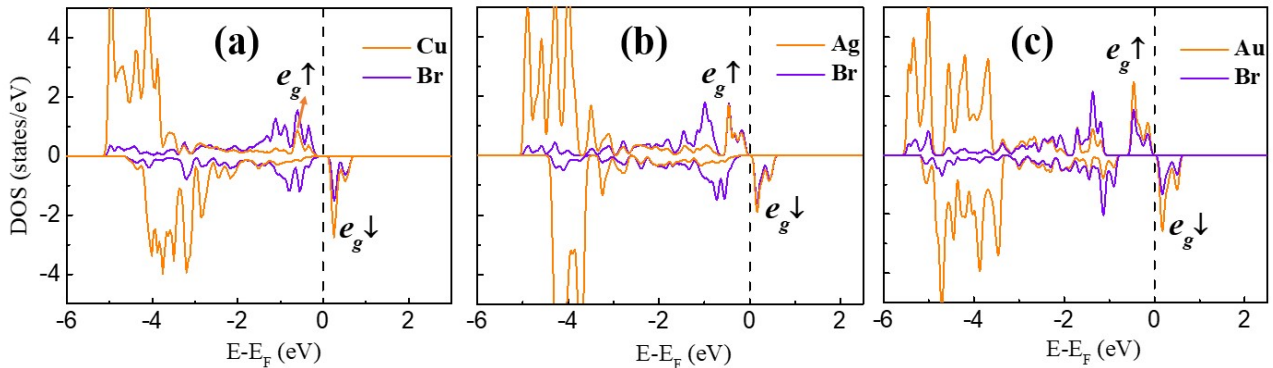


Fig. S4. The calculated partial DOSs of the (a) CuBr<sub>3</sub>, (b) AgBr<sub>3</sub>, and (c) AuBr<sub>3</sub> monolayers. The small up and down arrows express the spin-up and spin-down states, respectively.

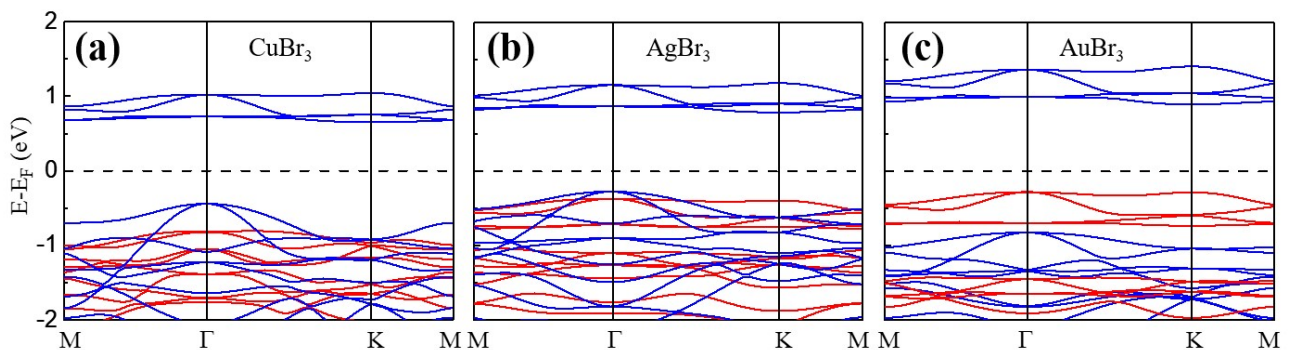


Fig. S5. Band structures of the monolayer XBr<sub>3</sub> (X = Cu, Ag, Au) in FM states with HSE06 functional.

The red (blue) curves represent the spin-up (spin-down) bands.

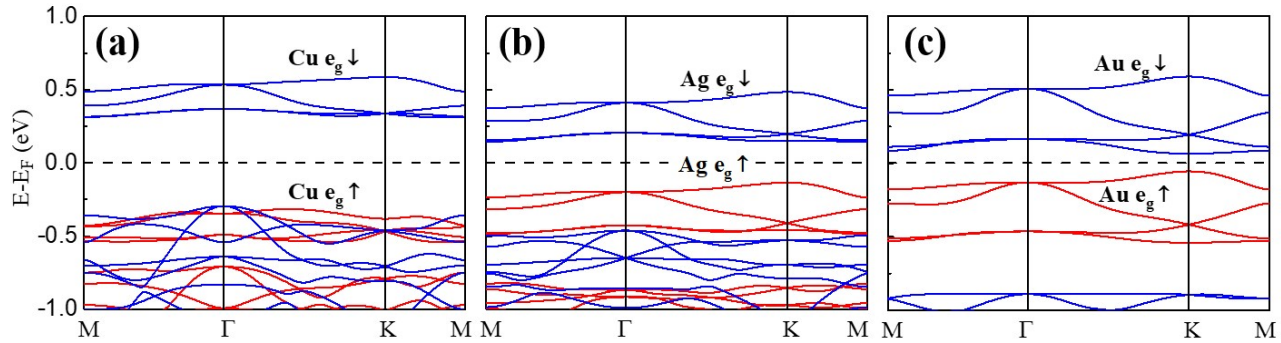


Fig. S6. Band structures of the monolayer  $X\text{Br}_3$  ( $X = \text{Cu}, \text{Ag}, \text{Au}$ ) in FM states under 5% tensile strain with GGA + U functional. The red (blue) curves represent the spin-up (spin-down) bands. The small up and down arrows express the spin-up and spin-down states, respectively.

## REFERENCES

- [1] P. Liu, F. Lu, M. Wu, X. Luo, Y. Cheng, X-W. Wang, W. Wang, W-H. Wang, H. Liu and K. Cho, Electronic structures and band alignments of monolayer metal trihalide semiconductors  $\text{MX}_3$ , *J. Mater. Chem. C*, 2017, **5**, 9066-9071.
- [2] Y. Zhou, H. Lu, X. Zu and F. Gao, Evidencing the existence of exciting half-metallicity in two-dimensional  $\text{TiCl}_3$  and  $\text{VCl}_3$  sheets, *Sci. Rep.*, 2016, **6**, 19407.
- [3] J. Geng, I. N. Chan, H. Ai, K. H. Lo, Y. Kawazoe, K. W. Ng and H. Pan, Magnetic and electronic properties of 2D  $\text{TiX}_3$  ( $X = \text{F}, \text{Cl}, \text{Br}$  and  $\text{I}$ ), *Phys. Chem. Chem. Phys.*, 2020, **22**, 17632-17638.
- [4] J. He, S. Ma, P. Lyu and P. Nachtigall, Unusual Dirac half metallicity with intrinsic ferromagnetism in vanadium trihalide monolayers, *J. Mater. Chem. C*, 2016, **4**, 2518-2526.
- [5] J. Sun, X. Zhong, W. Cui, J. Shi, J. Hao, M. Xu and Y. Li, The intrinsic magnetism, quantum

anomalous Hall effect and Curie temperature in 2D transition metal trihalides, *Phys. Chem. Chem. Phys.*, 2020, **22**, 24292-2436.

[6] W. B. Zhang, Q. Qu, P. Zhu and C. H. Lam, Robust intrinsic ferromagnetism and half semiconductivity in stable two-dimensional single-layer chromium trihalides, *J. Mater. Chem. C*, 2015, **3**, 12457-12468.

[7] Q. Sun and N. Kioussis, Prediction of manganese trihalides as two-dimensional Dirac half-metals, *Phys. Rev. B*, 2018 **97**, 094408.

[8] T. Liu, N. Zhou, X. Li, G. Zhu, X. Wei and J. Cao, Prediction of colossal magnetocrystalline anisotropy for transition metal triiodides, *J. Phys. Condens. Matter*, 2019, **31**, 295801.

[9] S. S. Li, Y. P. Wang, S. J. Hu, D. Chen, C. W. Zhang and S. S. Yan, Robust half-metallicity in transition metal tribromide nanowires, *Nanoscale*, 2018, **10**, 15545-15552.

[10] J. He, X. Li, P. Lyu and P. Nachtigall, Near-room-temperature Chern insulator and Dirac spin-gapless semiconductor: nickel chloride monolayer, *Nanoscale*, 2017, **9**, 2246-2252.

[11] Z. Li, B. Zhou and C. Luan, Strain-tunable magnetic anisotropy in two-dimensional Dirac half-metals: nickel trihalides, *RSC Adv.*, 2019, **9**, 35614-35623.

[12] L. Liu, Z. Lin, J. Hu and X. Zhang, Full quantum search for high  $T_c$  two-dimensional van der Waals ferromagnetic semiconductors, *Nanoscale*, 2021, **13**, 8137-8145.

[13] Q. Huang, Y. Z. Huang, Q. R. Zheng and G. Su, Half-metallicity of monolayer transition metal halide zirconium trichloride, *J. U. Chin. Acad. Sci.*, 2018, **35**, 297-301.

[14] J. Y. Zhang, B. Zhao, C. Ma and Z. Q. Yang, Bipolar ferromagnetic semiconductors and doping-tuned room-temperature half-metallicity in monolayer MoX<sub>3</sub> (X = Cl, Br, I): An HSE06 study, *Phys. Rev. B*, 2021, **103**, 075433.

- [15] S. Sarikurt, Y. Kadioglu, F. Ersan, E. Vatansever, O.Ü. Aktürk, Y. Yüksel, Ü. Akinci and E. Aktürk, Electronic and magnetic properties of monolayer  $\alpha$ -RuCl<sub>3</sub>: a first-principles and Monte Carlo study, *Phys. Chem. Chem. Phys.*, 2018, **20**, 997-1004.
- [16] F. Ersan, E. Vatansever, S. Sarikurt, Y. Yüksel, Y. Kadioglu, H. D. Ozaydin, O. Ü. Aktürk, Ü. Akinci and E. Aktürk, Exploring the electronic and magnetic properties of new metal halides from bulk to two-dimensional monolayer: RuX<sub>3</sub> (X = Br, I), *J. Magn. Magn. Mater.*, 2019, **476**, 111-119.
- [17] C. Huang, J. Zhou, H. Wu, K. Deng, P. Jena and E. J. Kan, Quantum anomalous Hall effect in ferromagnetic transition metal halides, *Phys. Rev. B*, 2017, **95**, 045113.
- [18] Y. Kadioglu, I. Ozdemir, O. Ü. Aktürk, G. Gökoğlu, Ü. Akinci and E. Aktürk, Tuning the electronic structure of RhX<sub>3</sub> (X = Cl, Br, I) nonmagnetic monolayers: effects of charge-injection and external strain, *Phys. Chem. Chem. Phys.*, 2020, **22**, 4561-4573.
- [19] Y. P. Wang, S. Li, C. W. Zhang, S. F. Zhang, W. Ji, P. Li and P. Wang, High-temperature Dirac half-metal PdCl<sub>3</sub>: A promising candidate for realizing quantum anomalous Hall effect, *J. Mater. Chem. C*, 2018, **6**, 10284-10291.
- [20] J-Y. You, Z. Zhang, B. Gu and G. Su, Two-Dimensional Room-Temperature Ferromagnetic Semiconductors with Quantum Anomalous Hall Effect, *Phys. Rev. Appl.*, 2019, **12**, 024063.
- [21] Q. Sun and N. Kioussis, Intrinsic ferromagnetism and topological properties in two-dimensional rhenium halides, *Nanoscale*, 2019, **11**, 6101-6107.
- [22] X. L. Sheng and B. K. Nikolić, Monolayer of the 5d transition metal trichloride OsCl<sub>3</sub>: A playground for two-dimensional magnetism, room-temperature quantum anomalous Hall effect, and topological phase transitions, *Phys. Rev. B*, 2017, **95**, 201402(R).
- [23] B. G. Li, Y. F. Zheng, H. Cui, P. Wang, T. W. Zhou, D. D. Wang, H. Chen and H. K. Yuan, First-

principles investigation of a new 2D magnetic crystal: Ferromagnetic ordering and intrinsic half-metallicity, *J. Chem. Phys.*, 2020, **152**, 244704.

[24] J-Y. You, C. Chen, Z. Zhen, X-L. Sheng, S. A. Yang and G. Su, Two-dimensional Weyl half-semimetal and tunable quantum anomalous Hall effect, *Phys. Rev. B*, 2019, **100**, 064408.

[25] Z. Zhang, J. Shang, C. Jiang, A. Rasmida, W. Gao and T. Yu, Direct Photoluminescence Probing of Ferromagnetism in Monolayer Two-Dimensional CrBr<sub>3</sub>, *Nano Lett.*, 2019, **19**, 3138-3142.

[26] B. Huang, G. Clark, E. Navarro-Moratalla, D. R. Klein, R. Cheng, K. L. Seyler, D. Zhong, E. Schmidgall, M. A. McGuire, D. H. Cobden, W. Yao, D. Xiao, P. Jarillo-Herrero and X. D. Xu, Layer-dependent ferromagnetism in a van der Waals crystal down to the monolayer limit, *Nature*, 2017, **546**, 270-273.